Proceedings of the ASME 2020 Conference on Smart Materials, Adaptive Structures and Intelligent Systems
SMASIS2020
September 15, 2020, Virtual, Online

SMASIS2020-2330

DEVELOPMENT AND DEMONSTRATION OF AN ORDERLY RECRUITMENT VALVE FOR FLUIDIC ARTIFICIAL MUSCLES

Jeong Yong Kim[1], Nicholas Mazzoleni, Dheeraj Vemula, Matthew Bryant
North Carolina State University
Raleigh, NC

ABSTRACT

Variable recruitment fluidic artificial muscle (FAM) bundles consist of multiple FAMs arranged in motor units that are sequentially activated as load demand increases. The conventional configuration of a variable recruitment FAM bundle requires a valve for each motor unit, which is referred to as a multi-valve system (MVS). As each motor unit within the bundle is selectively recruited, this configuration is highly adaptable and flexible in performance. However, as the number of motor units increases, the valve network can become complex and heavy in its design. To decrease complexity and weight, the concept of an orderly recruitment valve (ORV) has been proposed and analyzed. The ORV allows multiple motor units to be controlled using a single valve that recruits and pressurizes all motor units. The ORV concept consists of a spool valve with multiple outlet ports and a motor unit connected to each port. A linear actuator controls the position of the spool, allowing fluid flow into each port in succession. Naturally, de-recruitment happens in reverse order. The objective of the ORV is to strike a balance between performance and compactness of design. The purpose of this paper is to present analytical modeling that can be used to understand the behavior and performance of an ORV system and develop an experimental proof-of-concept that illustrates the ORV operation in hardware. A pneumatic ORV prototype was constructed and used to actuate two FAMs sequentially, each representing a motor unit. The results demonstrate the ORV as a compact system with which a variable recruitment bundle with multiple recruitment states can be controlled.

Keywords: fluidic artificial muscle, McKibben actuators, variable recruitment.

INTRODUCTION

Fluidic artificial muscles (FAMs) were invented in the 1960s by Joseph McKibben as a musculoskeletal aid to his polio-stricken daughter [1]. The FAM consists of an elastomeric bladder surrounded by a helically wound braided sheath. When the bladder is filled with pressurized fluid, it radially expands, and the kinematic constraints imposed by the sheath force it to axially contract. FAMs have become a popular actuation choice in mobile robotics due to their compliant nature, low cost, and high force-to-weight ratio. FAMs were originally pneumatic, using pressurized air as the working fluid, but recently, increased attention has been given to the use of hydraulic artificial muscles, as greater efficiency can be obtained due to the incompressible nature of hydraulic fluid [2, 3].

Many models and experimental studies regarding the behavior of individual FAMs have already been established [4-8], but there are still ways to improve the performance, efficiency, and adaptability of fluidic artificial muscles by leveraging the concept of variable recruitment. A variable recruitment bundle is a configuration of FAMs in parallel that allows subsets of the bundle, referred to as motor units, to be activated sequentially to adaptively respond to varying load requirements. This control strategy originates from how the motor units in a mammalian muscle tissue are sequentially recruited from smallest to largest to provide fine control, minimize muscle fatigue, and increase efficiency during varying load needs. This is known as Henneman's size principle [9]. Previous research regarding the modelling and fabrication of variable recruitment bundles has shown that using variable recruitment can improve system efficiency across a larger operation space when compared to a single equivalent actuator (i.e., an actuator with the same cross-sectional area), specifically

[1] Contact author: jkim84@ncsu.edu

when lower force regimes are required [10, 11]. The intuition behind this is that for a single actuator, at low force regimes, more energy is lost trying to throttle the pressure to achieve the desired force. In variable recruitment, on the other hand, since total cross-sectional area (and therefore total force) is divided within discrete motor units, less throttling is required at lower force regimes. Conventional methods of throttling the pressure of FAMs within a variable recruitment bundle involve a common pressure supply and an independently controlled valve for each motor unit. A pressure supply consists of a pump, reservoir, and accumulator, each of which can be sized properly to fit the application. A system consisting of *n* FAMs requires *n* valves to operate. However, in many applications like mobile robots or human exoskeletons, space and mass are limited, making multiple valves undesirable or impractical. The concept of an orderly recruitment valve (ORV) has been proposed in a prior work [12] as a solution to decrease the complexity of a variable recruitment system with multiple FAMs. An ORV primarily consists of a cylindrical body and a spool. For the purpose of demonstrating its conceptual operation, the design of an ORV capable of recruiting and controlling two motor units is illustrated in FIGURE 1. There are four ports required. The rightmost and leftmost ports are connected to the pressure source and reservoir, respectively. The two middle ports are for the two motor units for which the pressure will be controlled. This paper will discuss the development of an analytical model and an experimental proof-of-concept and hardware implementation of the ORV.

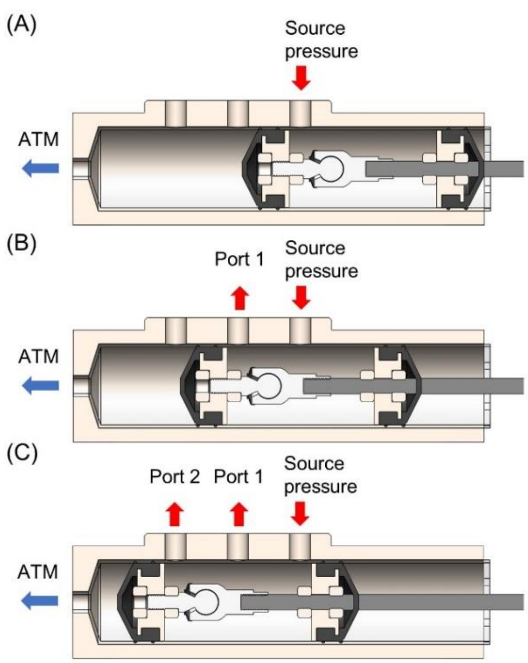

FIGURE 1: CROSS-SECTIONAL VIEW OF ORV AND SPOOL POSITIONS AT THE (A) NEUTRAL STATE WITH BOTH MOTOR UNITS INACTIVE, (B) FIRST MOTOR UNIT ACTIVE (C) BOTH FIRST AND SECONDMOTOR UNITS ACTIVE

ORV CONCEPT DEVELOPMENT AND MODELING

Before we discuss the hardware implementation of the ORV, it is important to understand some of the theoretical background information that motivated the development of an ORV in hardware, first presented by Vemula and Bryant in 2019 [12]. Although there is no theoretical limit to the number of motor units that can be pressurized by the ORV, for this analysis we will consider two motor units consisting of one FAM each for simplicity. As the ORV spool travels along the length of the valve, it sequentially opens FAM ports 1 and then 2 to the supply pressure. When ports 1 and 2 are both open, the ORV experiences a phenomenon known as crossflow, which is a flow coupling behavior between the two ports. Assuming incompressible working fluid (i.e. hydraulic operation), the flow equations for this behavior are given by:

$$Q_{FAM1}^{ORV} = c_v x_{v,1}\sqrt{|P_s - P_1|}sgn(P_s - P_1) - Q_{cf} \tag{1}$$

where c_v is the valve flow coefficient, P_s is the supply pressure, $x_{v,1}$ is the FAM port 1 opening, P_1 is the pressure of fluid in FAM port 1, and Q_{cf} is a crossflow term. The valve coefficient is given by [13]:

$$c_v = \frac{Q_N}{\sqrt{\Delta p_N/2}}\frac{1}{x_{v,max}} \tag{2}$$

where Q_N and Δp_N are the nominal flow rate and pressure drop for the valve and $x_{v,max}$ is the maximum valve stroke.

We can express the flow equation for FAM port 2 in a similar manner:

$$Q_{FAM2}^{ORV} = c_v x_{v,2}\sqrt{|P_s - P_2|}sgn(P_s - P_2) + Q_{cf} \tag{3}$$

The crossflow equation between ports 1 and 2 is given by:

$$Q_{cf} = c_v \max(x_{v,1}, x_{v,2})\sqrt{|P_1 - P_2|}sgn(P_1 - P_2) \tag{4}$$

The difference between the ORV equations and the equations for a multi-valve system (MVS) is the presence of this crossflow term that creates coupling between the flow of ports 1 and 2. In order to calculate valve flow rates, we need to know the valve spool position, which can be simulated using a second-order differential equation [13]:

$$\frac{1}{\omega_v^2}\ddot{x}_v + \frac{2D_v}{\omega_v}\dot{x}_v + x_v + f_{hs}sign(\dot{x}_v) = K_v u_v \tag{5}$$

where ω_v is valve natural frequency, K_v is valve gain, u_v is valve control input signal, D_v is valve damping coefficient, and f_{hs} is valve hysteresis. Simulating this differential equation for valve position allows us to calculate ORV flowrate to the different FAM ports as a function of valve position. We can then use these ORV flow rates to calculate the pressure, force, and strain dynamics of the FAMs attached to each ORV port. If we assume an ideal FAM model, as developed by Tondu and Lopez [4], we can express the volume consumed by a FAM as a function of strain:

$$V_m = \pi r_0^2 l_0 \left[b\left(1-\frac{x_m}{l_0}\right) - \frac{a}{3}\left(1-\frac{x_m}{l_0}\right)^3 \right] \tag{6}$$

where r_0 and l_0 are the initial FAM radius and length, x_m is the FAM strain, and a and b are geometric parameters, both functions of initial braid angle α_0, given by:

$$a = \frac{3}{tan^2\alpha_0} \tag{7}$$

$$b = \frac{1}{sin^2\alpha_0} \tag{8}$$

The FAM force can be derived using a virtual work balance:

$$PdV_m = F_m dx_m \tag{9}$$

This can be rearranged to solve for muscle force F_m:

$$F_m = P\frac{dV_m}{dx_m} \tag{10}$$

Our final expression for muscle force is given by:

$$F_m = \pi r_0^2 P\left[a\left(1-\frac{x_m}{l_0}\right)^2 - b\right] \tag{11}$$

We can simulate the FAM force dynamics during the actuation of the ORV by considering the pressure dynamics of the individual FAM. These dynamics are assumed to be the result of isothermal compression of the fluid within the FAM, given by the following equation:

$$\frac{dP}{dt} = \frac{1}{\beta}\frac{Q-\dot{V}_m}{V_m} \tag{12}$$

where β is the compressibility of the fluid. The time rate of change of fluid volume of the FAM is given by:

$$\dot{V}_m = \left[a\left(1-\frac{x_m}{l_0}\right)^2 - b\right]\dot{x}_m \tag{13}$$

The ORV flow equations and spool position dynamics can be used to simulate the FAM pressure dynamics, and therefore the FAM force/strain dynamics.

To analytically demonstrate the functionality of the ORV at its most basic level, we will consider the transient pressure behavior of a free-contracting two-FAM system with a prescribed valve spool travel and fixed spool travel rate. The term 'free-contracting' means that there is no load attached to the FAMs. In order to analyze strain vs. time behavior of the system, we use a corrected model [14] that accounts for pressure-dependent free-contracting behavior using a curve-fit polynomial that depends on the specific bladder geometry and material of a given FAM. The polynomial we have used in this analysis corresponds to one used by Jenkins et al. [15]:

$$\begin{aligned}\varepsilon_{free} = (&1.242\times10^{-18}P^3 - 2.167\times10^{-12}P^2 \\ &+1.342\times10^{-6}P - 0.0377\end{aligned} \tag{14}$$

We can use this curve-fit for ε_{free} to calculate each muscle displacement x_m:

$$x_m = l_0\varepsilon_{free}(P) \tag{15}$$

To find the time derivative of x_m, we use the chain rule:

$$\dot{x}_m = \left(\frac{dx_m}{dP}\right)\left(\frac{dP}{dt}\right) \tag{16}$$

We can substitute this expression into the equation for $\dot{V}_m$:

$$\dot{V}_m = \left[a\left(1-\frac{x_m}{l_0}\right)^2 - b\right]\left(\frac{dx_m}{dP}\right)\left(\frac{dP}{dt}\right) = \gamma\left(\frac{dP}{dt}\right) \tag{17}$$

where γ is used to group terms together for simplicity. Substituting this into equation (12) and rearranging, we get:

$$\frac{dP}{dt} = \frac{Q}{\beta V_m + \gamma} \tag{18}$$

This differential equation can be used for each FAM to simulate pressure vs. time and free strain vs. time assuming a fixed linear spool travel rate.

FIGURE 2 shows the plots for pressure vs. time for when crossflow effects are neglected and when crossflow effects are considered. Note that in both plots, pressure has been normalized by source pressure, so the maximum value is unity. For both cases, it is assumed that the spool is critically lapped, meaning that the width between the two FAM ports is identical to the spool width and the width of the two FAM ports. In addition, all of the valve parameters and specifications were taken from the datasheet of a MOOG G761 industrial grade electrohydraulic servo valve.

We see that when crossflow effects are considered, the pressure in FAM 1 drops significantly when the FAM 2 port is opened. This is an important factor that must be considered when designing a variable recruitment system that uses an ORV, as in an MVS system, this crossflow effect would not be present [12]. To calculate the free strain vs. time from these plots, we would simply use the pressure values obtained from this simulation and substitute into the curve-fit for pressure-dependent free strain. After constructing our proof-of-concept ORV, our goal was to experimentally reproduce these transient pressure plots on a qualitative level, since the exact valve parameters of our proof-of-concept ORV design would not be known.

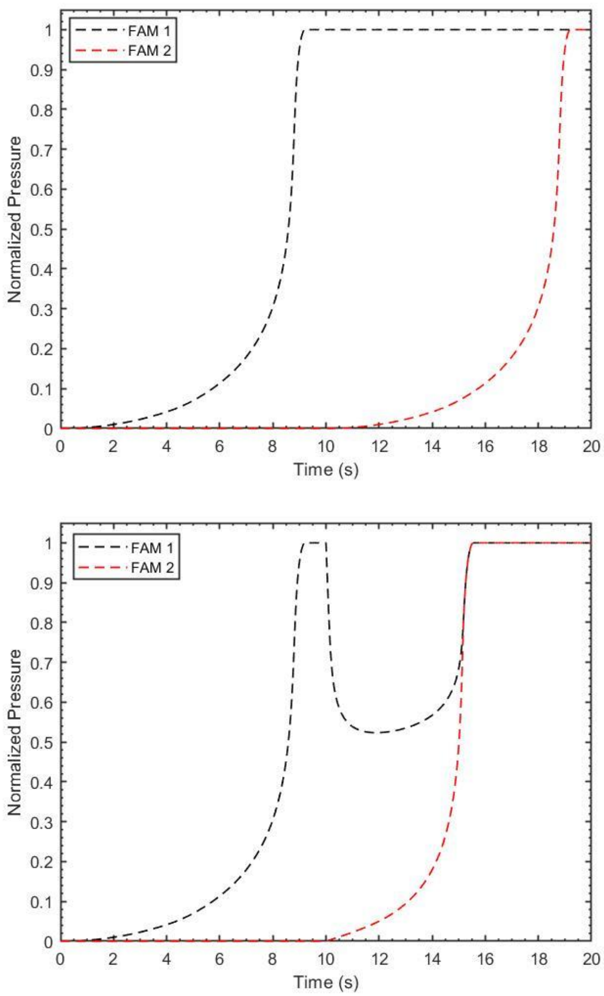

FIGURE 2: (TOP) NORMALIZED PRESSURE VS. TIME PLOT FOR FAM 1 AND FAM 2, NEGLECTING CROSSFLOW EFFECTS WITH FIXED SPOOL TRAVEL RATE OF 2.16 MM/S. (BOTTOM) NORMALIZED PRESSURE VS. TIME PLOT FOR FAM 1 AND FAM 2 CONSIDERING CROSSFLOW EFFECTS WITH FIXED SPOOL TRAVEL RATE OF 2.16 MM/S.

ORV DESIGN CONSIDERATIONS

To demonstrate the working principle of an orderly recruitment valve, we developed and tested an in-house prototype. The design proposed in prior work highly resembles a spool valve. The manufacturing practice concerning the quality of a spool valve (i.e., tolerances required for a sufficient sealing mechanism while minimizing friction in the piston movement) is already well established in the industry. However, as a preliminary proof-of-concept, the ORV prototype was made with a combination of off-the-shelf components and 3D-printed parts.

FIGURE 3 shows a cross-sectional view of the ORV with the parts labeled. The ports for the source pressure and the two motor units are indicated in FIGURE 3 from right to left. The leftmost port can be vented for a pneumatic system or connected to a reservoir for a hydraulic system A key component in any pressurized setup is the sealing mechanism. The ORV requires a seal between each spool and the inner surface of the chamber. To create a reliable seal for the prototype, we used parts from a syringe because they were easy to acquire and modify. The syringe body provided the smooth inner surface that was not possible from a 3D-printed part. The rubber caps of the syringe pistons were used on the outside end of each piston to ensure a sealing mechanism that could operate up to 50 psi. The syringe body was tightly fit into a 3D-printed chassis and the gap was sealed using epoxy. The purpose of the body was to provide a solid interface between the inner chamber and fittings used to connect the ORV with the source pressure and FAMs. To ensure a tight seal, a revolute joint was used to connect the two spools to account for any misalignment that would cause a gap between the rubber cap and chamber wall.

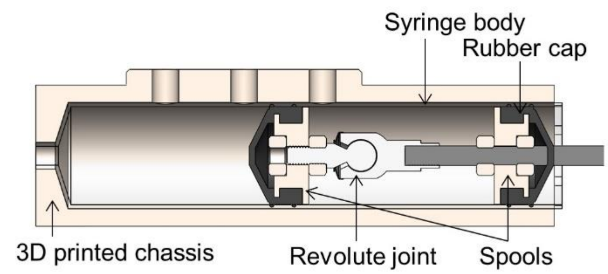

FIGURE 3: CROSS-SECTIONAL VIEW OF ORV WITH INTERNAL PARTS LABELED

PROOF-OF-CONCEPT DEMONSTRATIONS

We devised a simple experiment to demonstrate the ability of the ORV to sequentially recruit two different motor units and observe the transient pressure behavior shown in the analytical section of the paper. The ORV was tested using two FAMs, each representing a motor unit. One end of each FAM was connected to a rigid plate and the other ends were free to contract without any load. The FAMs were made to be identical with an initial braid angle of 33° and bladder inner radius of 4.76 mm. The spool rod of the ORV was connected to the ball nut of a ball screw setup, which was driven by a stepper motor. Pressure transducers were connected to each FAM to measure the change in pressure. The strain of each FAM was measured from a video taken by a camera. A regulator was used to set the source pressure to a desired value. Although the experimental results presented in this paper are limited to a pneumatic system, future studies will involve the use of a hydraulic power supply for which a blast shield was designed to protect the user and equipment from potential failures of the FAMs or the ORV. For preliminary results, there was no closed-loop feedback used for the control of source pressure, spool position or FAM strain. A Labview DAQ was used in the open-loop control of the stepper motor and pressure measurements for each FAM to ensure that they were synchronized.

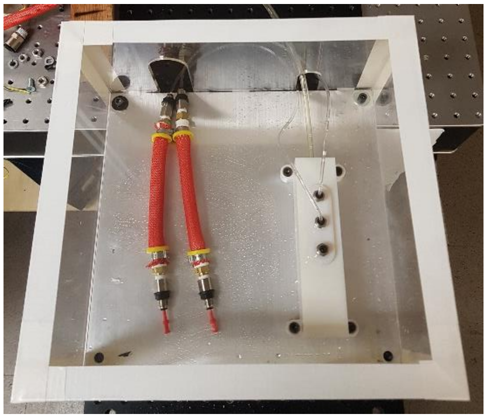

FIGURE 4: THE ORV TEST SETUP PLACED IN ITS BLAST SHIELD IN PREPERATION FOR HYDRAULIC TESTING

FIGURE 5 shows the pressure measurements for FAM 1 and FAM 2 as the spool is actuated to move along the valve at a constant rate. The source pressure was set to 138 kPa (20 psi). As the spool moves across, the ports connected to FAM 1 and FAM 2 open sequentially, activating the FAMs. As the port connected to FAM 1 is opened, the pressure initially starts at zero and reaches a constant value as the port is fully opened. As the second port is opened, the pressure for FAM 2 rises until it reaches a constant value. Although, they fall short of a full validation of this behavior, these results demonstrate the qualitative behavior shown in FIGURE 2. This is because the dynamic effects such as crossflow are less evident in this experiment since the working fluid was compressed air. Contrary to the simulation result that shows a decrease in FAM 1 pressure, experimental results show the opposite behavior. The pressure of FAM 1 starts increasing until both FAMs reach a new equilibrium. One setback of this set of experiments is that the source pressure was controlled using a regulator which may have allowed it to fluctuate as the FAMs were activated. Future work will involve a transducer to monitor the closed-loop control of the source pressure.

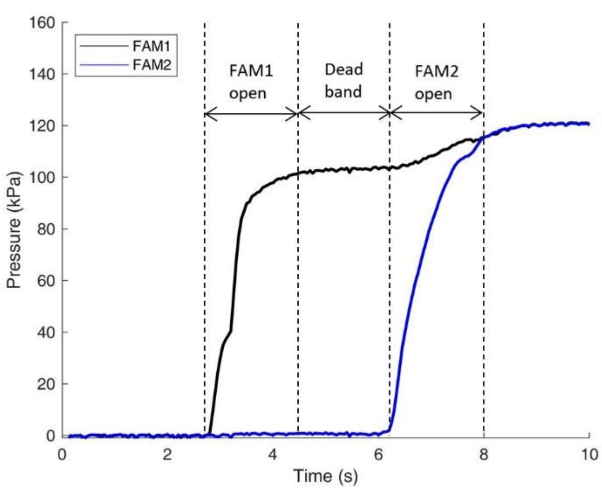

FIGURE 5: PRESSURE MEASUREMENTS SHOW THE SEQUENTIAL ACTIVATION OF FAM 1 AND FAM 2

A comparison of the measured and theoretical free strain is illustrated in FIGURE 6. Theoretical free strain, shown in solid lines, is computed using a quasi-static model of FAMs. Among many models in the literature, a virtual work-based model developed by Klute et al. [5] that incorporates the hyperelastic behavior of the bladder was used. The elastic force of the bladder is critical in capturing the pressure dependent free strain of FAMs. The curve-fit free strain function used in the analytical section could not be used for the FAMs in this experiment, since they had different characteristics from the ones used to generate that curve fit. We observed that theoretical values are greater than that of measured values, which is expected when using this model as it tends to be accurate in predicting blocked force but overpredicts free strain. Despite discrepancies in the strain values, the simulation and measured strain demonstrate the ability of the ORV to sequentially activate two FAMs.

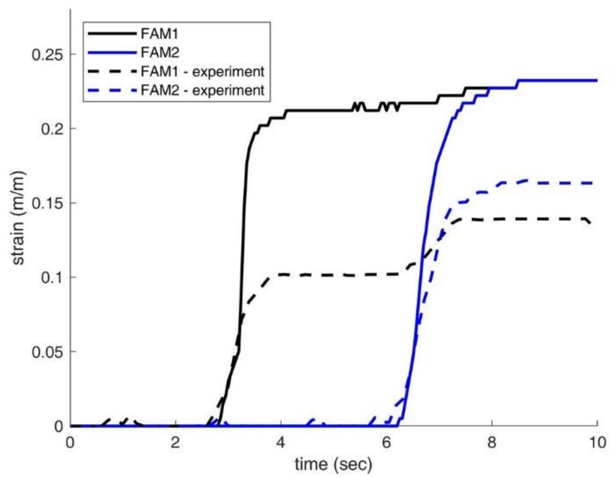

FIGURE 6: COMPARISON OF THEORETICAL STRAIN AND MEASURED STRAIN OF FAM 1 AND FAM 2

CONCLUSION

In this study, an orderly recruitment valve (ORV) was designed and tested to demonstrate its feasibility. Compared to the MVS configuration, which requires one valve for each motor unit, the ORV design enables multiple motor units to be sequentially activated with one valve. The ORV reduces the complexity of the fluid power circuit by reducing the number of valves needed. However, it also assumes recruitment states to be activated in a prescribed sequence, while the MVS offers the additional flexibility to adjust recruitment sequence during operation. This study provides preliminary results that successfully demonstrate the ability of the ORV to sequentially recruit FAMs in a manner similar to that predicted by the analytical model of the ORV. Moving forward, a direct comparison of the ORV to an equivalent MVS will better highlight trade-offs associated with the ORV, such as deadband and crossflow.

ACKNOWLEDGEMENTS

This work was supported primarily by the Faculty Early Career Development Program (CAREER) of the National Science Foundation under NSF Award Number 1845203 and Program Manager Irina Dolinskaya. Additionally, this material is based upon work supported by the National Science Foundation Graduate Research Fellowship Program under Grant No. 1650114. Any Opinions, findings and conclusions or recommendations expressed in this material are those of the author(s) and do not necessarily reflect those of the National Science Foundation.

REFERENCES

[1] Tondu, B., 2012, "Modelling of the McKibben Artificial Muscle: A Review," Journal of Intelligent Material Systems and Structures, 23(3) pp. 225-253.

[2] Tiwari, R., Meller, M. A., Wajcs, K. B., 2012, "Hydraulic Artificial Muscles," Journal of Intelligent Material Systems and Structures, 23(3) pp. 301-312.

[3] Meller, M. A., Bryant, M., and Garcia, E., 2014, "Reconsidering the McKibben Muscle: Energetics, Operating Fluid, and Bladder Material," Journal of Intelligent Material Systems and Structures, 25(18) pp. 2276-2293.

[4] Tondu, B., and Lopez, P., 2000, "Modeling and control of McKibben artificial muscle robot actuators," in IEEE Control Systems Magazine, 20(2) pp. 15-38.

[5] Klute, G. K., and Hannaford, B., 2000, "Accounting for Elastic Energy Storage in McKibben Artificial Muscle Actuators," Journal of Dynamic Systems, Measurement, and Control, 122(2) pp. 386-388.

[6] Kothera, C. S., Jangid, M., Sirohi, J., 2009, "Experimental Characterization and Static Modeling of McKibben Actuators," Journal of Mechanical Design, 131(9) pp. 91010.

[7] Ball, E., and Garcia, E. 2016, "Effects of Bladder Geometry in Pneumatic Artificial Muscles." ASME. J. Med. Devices, 10(4) pp. 041001.

[8] Yu, Z., Pillsbury, T., Wang, G., 2019, "Hyperelastic Analysis of Pneumatic Artificial Muscle with Filament-Wound Sleeve and Coated Outer Layer," Smart Materials and Structures, **28**(10) pp. 105019.

[9] Henneman, E., 1965 "Excitability and inhibitability of motoneurons of different sizes," Journal of neurophysiology (0022-3077), 28 (3) p. 599.

[10] Bryant, M., Meller, M. A., and Garcia, E., 2014, "Variable Recruitment Fluidic Artificial Muscles: Modeling and Experiments," Smart Materials and Structures, 23(7) pp. 74009.

[11] DeLaHunt, S. A., Pillsbury, T. E., and Wereley, N. M., 2016, "Variable Recruitment in Bundles of Miniature Pneumatic Artificial Muscles," Bioinspiration & Biomimetics, 11(5) pp. 056014.

[12] Vemula, D., and Bryant, M., 2019, "Bio-inspired orderly recruitment valve for fluidic artificial muscles," Proc. SPIE 10965, Bioinspiration, Biomimetics, and Bioreplication IX, pp. 109650.

[13] Jelali, M. and Kroll, A., 2012, [Hydraulic servo-systems: modelling, identi_cation and control], Springer Science & Business Media.

[14] Meller, M., Chipka, J., Volkov, A., 2016, "Improving Actuation Efficiency through Variable Recruitment Hydraulic McKibben Muscles: Modeling, Orderly Recruitment Control, and Experiments," Bioinspiration & Biomimetics, 11(6) pp. 065004.

[15] Jenkins, T. E., Chapman, E. M., and Bryant, M., 2016, "Bio-Inspired Online Variable Recruitment Control of Fluidic Artificial Muscles," Smart Materials and Structures, 25(12) pp. 125016.

